Comparison of five performance metrics applied to five WEC concepts

Ronan Costello, Morgan Jones and Ben Kennedy

Abstract—**In early stage technology design for wave energy conversion, comparison of alternative competing concepts is a key activity in determining the relative merits of candidate concepts. Careful selection of the measures ("metrics") used in such a comparison is also of utmost importance since alternative metrics can be shown to give contradicting indications. To develop high performing wave energy technology it is vital that R&D strategy is informed by high quality execution of the concept comparison and metric selection activities.**

This paper presents an analysis of five generic heaving wave energy converter (WEC) concepts drawn from a survey of current and past WEC technology. For each of the five concepts we calculate five metrics also drawn from previously published work. The analysis utilises hydrodynamics based on linear potential flow. The relative merits of the selected devices and the selected metrics are discussed in the context of the modelling methods used.

Keywords—. **Dynamics, heave mode, numerical simulation, optimization, power production assessment, wave energy converter.**

I. Introduction

A focus of this analysis is to explore methodologies suitable for very early stage wave energy research. The metrics used in concept comparison at very early stage can have a strong impact on the subsequent R&D direction so careful, justified and informed selection of these metrics is warranted [1].

A further objective of this work is to make a comparative assessment of the selected concepts rather than a detailed assessment of any specific instance of the concepts. To address this objective a parameter study is undertaken for each of the selected devices so that the assessment is applied to many instances rather than a single instance of each design. This approach provides an overview of the performance of a wide range of designs within each concept. Two advantages of assessing such a large number of designs are, firstly, that the true potential of a concept is more likely to be discovered since even high potential concepts may yield low performing point estimates for certain geometry/control combinations, and, secondly, that the properties of the metrics used can be better understood.

There is necessarily a trade-off between the breadth and the depth of the analysis that is possible within given time or budget constraints. Nevertheless, the broader analysis with many design instances resulting from parameter studies and optimisations is a better basis for early stage R&D decision making than a single high detail point estimate is.

In the literature there is a lack of multi concept comparative studies where common methods and metrics are applied to multiple devices, [2] being a notable exception. In general there is also lack of comparative studies that focus on meaningful parameter studies or optimisations and avoid focusing on a single design instance of each concept. Most often, in optimisation studies the effect of choice of metric of objective function is also inadequately considered.

The relevance of the metrics reported in [1] and [2] seem obvious yet the validity of these has not been formally established. This paper aims to present these metrics for a wider range of designs than has previously been available with a view to providing information that might in time contribute to judgements about the validity and the relative merits of the metrics.

A. Concept Selection

Two of the key attributes of a WEC that are commonly referred to in WEC classification are firstly the principle mode of rigid body motion from which power is absorbed and secondly the means of providing a reaction force for the power take off machinery [3]. A previous survey of the public domain information on current WEC designs was undertaken in [4]. This paper focuses on devices using the heave mode of motion and a range of different reaction types. Amongst the various heaving concepts, five generic device types were selected as representative of commonly chosen design approaches. These were:

- Surface piercing buoy with seabed reaction
- Sub-surface buoy with seabed reaction
- Free-floating buoy with sub-surface reaction plate
- Free-floating buoy with internal reaction mass
- Free-floating, two-body axisymmetric WEC

Devices falling within one or other of these categories made up a large share of the surveyed technologies [5]. Further review of the history of WEC development

1708 Wave Hydrodynamic modelling
R. Costello is with Wave Venture Ltd., Penstraze Business Centre, Cornwall, UK (email: ronan@wave-venture.com).
M. Jones is with Wave Venture Ltd., Penstraze Business Centre, Cornwall, UK (email: morgan.jones@wave-venture.com).
B. Kennedy is with Wave Venture Ltd., Penstraze Business Centre, Cornwall, UK (email: ben@wave-venture.com).

indicates that the heaving buoy is a common initial design that appeals to many early stage inventors.

II. Methodology

A model comprising hydrodynamics based on linear potential flow is assembled for the five devices. A parameter study is undertaken to investigate the performance of a range of combinations of geometrical parameters. In each case the annual average power performance is calculated using a scatter diagram method and the other metrics are calculated using this annual average power.

The model is a frequency domain calculation following the theory as described in [6, 7] and implementation as detailed in [8], with the implicit assumption of small body motions. A wetted surface mesh was prepared for each of the selected generic devices. Hydrodynamic coefficients were calculated using a linearised boundary element method (in this case the NEMOH open source BEM solver [9]). Constraints due to joints between the bodies were represented using the linearized joint co-ordinate method approach [8].

The inertia properties were set in each case so that the bodies are neutrally buoyant (in the case of the internal reaction mass device the device was neutrally buoyant considering the mass of both bodies combined). The frequency domain equations of motion were then solved to determine body behaviour and WEC power performance for the modelled design instances.

To increase the likelihood that a comparison is made between the high performance instances of each device, (acknowledging that we do not know which metric high performance might be measured by) a parameter study is run to generate many combinations of geometrical parameters.

In each case the power take-off (PTO) system was assumed to be a linear damper; there was no consideration given to PTO design or constraints, as this was a study of generic concepts. In each case the PTO damping was set to the absolute value of the intrinsic impedance of the system, which is the optimum for a PTO mechanism with zero stiffness [10].

		Average Annual Power (kW)										
		Peak Period Tp (s)										
		3.5	4.5	5.5	6.5	7.5	8.5	9.5	10.5	11.5	12.5	13.5
Significant Wave Height (m)	0.5	0.007	0.023	0.014	0.020	0.041	0.052	0.038	0.020	0.007	0.003	0.001
	1.5	0.000	0.023	0.073	0.057	0.029	0.040	0.056	0.065	0.052	0.027	0.009
	2.5	0.000	0.000	0.005	0.044	0.039	0.017	0.014	0.022	0.028	0.026	0.017
	3.5	0.000	0.000	0.000	0.002	0.017	0.021	0.010	0.008	0.009	0.009	0.009
	4.5	0.000	0.000	0.000	0.000	0.001	0.007	0.009	0.005	0.003	0.003	0.003
	5.5	0.000	0.000	0.000	0.000	0.000	0.000	0.002	0.004	0.002	0.001	0.001
	6.5	0.000	0.000	0.000	0.000	0.000	0.000	0.000	0.001	0.001	0.001	0.000

Fig. 1. Normalized Probability of Occurrence of Sea States

The wave climate used during this modelling is based on an average unidirectional wave spectrum derived from ECMWF data with a location set close to the Wave Hub Demo site, Cornwall [11]. The scatter diagram occurrence matrix is shown in Fig. 1.

III. The Metrics

The metrics considered in this paper are drawn from [1], [2].

A. Annual Average Power

The annual average power (AAP) is one of the most important metrics for a WEC; the AAP is a direct determinant of revenue for a wave farm and therefore a key indicator of commercial performance. It should be noted, however, that although a higher *average* power indicates greater energy production, *peak* power is largely irrelevant to remuneration and therefore caution should be exercised in using power as a metric. The principal shortcoming of this metric is that it does not represent costs of the system.

B. Annual Average Power p.u. Surface Area

Along with potential revenue, a key indicator of commercial viability of a WEC is the associated manufacturing costs. This metric addresses the shortcoming of Metric A by including the device surface area as a surrogate for structural cost. The ratio of average annual power to surface area therefore approximates to the ratio of revenue to manufacturing costs, with a higher ratio being desirable.

This metric is possibly most relevant to devices manufactured from high strength materials (e.g. steel or glass reinforced plastics) where the structure is reasonably well approximated as a thin shell and cost is better correlated with the surface area than displacement.

The detail of actual manufacturing costs and the relative prices of manufacture per surface area and power will complicate this picture. It is not suggested that this is used as a measure of full wave farm economics, merely of the contribution to this of WEC cost.

C. Annual Average Power p.u. displacement

Similarly to Metric B the displacement of a body is representative of its size and mass. This can again be related to cost, with larger and heavier bodies being costlier and more difficult to manufacture and install. This metric is possibly most relevant to devices manufactured from low strength materials such as concrete where the structural sections are thick and not well approximated as a thin shell and where the structural mass is correlated with the displacement.

D. Annual Average Power p.u. RMS PTO stroke

In devices with linear PTO mechanisms (as in virtually all heaving devices) the PTO stroke is necessarily limited; design changes to increase the stroke beyond a certain limit will not be justifiable given diminishing gains in the power capture (for example see [10], Section 2.4.5.4). The PTO stroke is an indicator of cost, longer strokes increase the size and complexity of both the PTO mechanism and the device hull structure. This metric will be most relevant to devices where the structural cost is driven by

the PTO stroke or where the PTO size is a dominant cost driver. No constraint was applied to device motion.

E. Annual Average Power p.u. RMS PTO force

PTO systems subject to higher forces require more costly PTO equipment and greater mechanical reinforcement of the hull structure. PTO forces may therefore be a valid cost driver for wave energy devices and potentially a valid surrogate for device cost to use in metrics. AAP per unit PTO force is most relevant to devices where the device cost is dominated by costs of PTO force provision and/or costs of reinforcing the hull structure to accommodate PTO forces.

IV. DEVICES

Fig. 2 shows the five devices selected for the analysis in schematic. The five devices are:

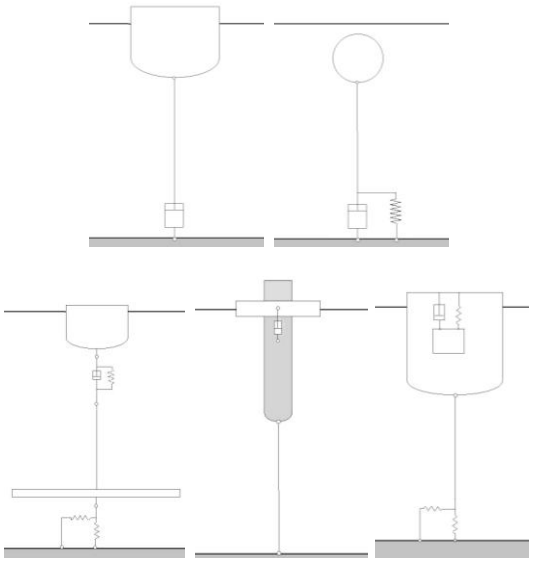

Fig. 2. Schematic of five device types (a) surface piercing buoy with seabed reaction (b) submerged buoy with seabed reaction (c) free-floating buoy with subsurface reaction plate (d) free-floating, two-body axisymmetric (e) surface piercing buoy with internal reaction mass.

F. Surface piercing bottom reacting heaving buoy

Device A is a generic heaving buoy. The geometry is a vertical cylinder with a rounded lower end. Radii between 2.5 m and 10 m were trialled, for draft: radius ratios of 0.25, 0.33, 0.50, 0.66, 0.75 and 1.

The WEC uses an absolute reference frame with PTO reaction forces passing through the anchor to the sea bed. The PTO is modelled as a damper i.e. settable damping and zero stiffness. The absorber does not have an inherent end stop but the PTO mechanism may introduce an end stop. Hydraulic or linear generator systems for example will introduce end stops while a winch or similar PTO can have arbitrarily long stroke and effectively avoid end stops. The mooring is a single vertical tether joining the buoy to the PTO, in practice reserve moorings or secondary moorings may be needed but will have no impact on the dynamics and are neglected here. This body will behave as a quasi-point absorber [12]. Manipulation of the WEC's natural frequency is achieved by tailoring the ratio of surface piercing area to displaced mass, this ratio is approximately equal to the draft of the hull.

G. Sub-surface bottom reacting heaving buoy

Device B is a generic submerged buoy. The geometry is an ellipsoid, with height less than or equal to radius. Radii between 2.5 m and 12.5 m were trialled, with height: radius ratios of 0.25, 0.33, 0.5, 0.66, 0.75 and 1. The ellipsoid centre is submerged to 15 m and the ellipsoid radius and height are varied in the parameter study. The PTO reacts against the seabed through an anchor, and is modelled as a damper, with adjustable damping and zero stiffness. There was no inherent end stop, but the PTO system may introduce one. The mooring is a single vertical tether joining buoy and PTO; reserve moorings and secondary moorings were neglected as they have no effect on the dynamics. The energy capture of submerged buoys is potentially limited as they operate beneath the most energetic part of the sea surface - but there are advantages to submersion such as reduced visual impact and lower exposure to extreme waves. In this case movement was limited to the heave direction as taking power from the surge requires a more complex, non-vertical mooring. Submergence tends to reduce the bandwidth of a converter [13].

H. Surface piercing buoy with subsurface reaction plate

Device C shared a geometry with Device A, with a buoy radius of 10 m and a draft of 2.5 m. In this case the PTO forces react against a subsurface reaction plate, which is circular, 0.2 m in height and centred beneath the surface piercing buoy. The plate radius was studied in the range from 2.5 m to 20 m, and the depth of submergence between 20 m and 50 m. This plate is then slack moored to the seabed. The submerged plate replaces the absolute reference used in device A & B with a large added inertia in heave. The PTO is connected by a single vertical tether between the buoy and the reaction plate. In practice since this device is a 2 body device it will most likely have end stops irrespective of PTO machinery selected.

I. Surface piercing buoy with internal reaction mass

Device D again shares a geometry with Device A & C i.e. a semi-submerged vertical cylinder with a rounded lower end, but in this case contains an internal moving mass in the form of a vertical cylinder with flat ends. Two external buoy geometries were used; both of radius 10 m, one of draft 5 m and one of draft 7.5 m. The internal mass remains relatively stationary as the external buoy moves, and its inertia provided reaction for the PTO system. In this case, the PTO was on the vertical axis of both the buoy and the internal mass and attached between the two. End stops must be assumed due to the constraint

that the mass remain internal. The moorings were neglected.

J. *Surface piercing two-body self-reacting buoy*

Device E is a surface piercing, long vertical cylinder of radius 4 m and draft 12 m, with a rounded lower end, surrounded by a vertically sided ring. The radius of the ring was varied between 6 m and 10 m and ratios of height: radius of 0.25, 0.50 and 0.75. The WEC is self-reacting, with the PTO joined between the cylinder and the ring. The device is slack moored.

V. RESULTS

K. *Surface piercing buoy with seabed reaction*

Fig. 3 shows the nature of the dependence of the power on the PTO damping. It is apparent from Fig. 3 that as could be expected both the optimal PTO damping and the average annual power will also change with the geometry of the buoy. In each case, in the following results, the optimal damping was selected for each geometry.

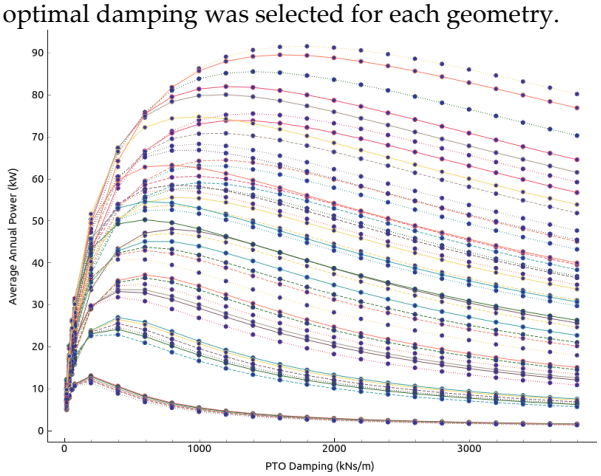

Fig. 3. Average Annual Power (kW) variation with PTO damping for different buoy geometries.

Fig. 4 shows the AAP for a range of geometries. The AAP increases with increasing buoy radius and decreases with increasing buoy draft; wider but shallower buoys have the greatest average annual power. This trend is explained by the increased wave forcing of these geometries due to a larger excitation force provided by the larger radii increasing the area for pressure to act on and higher pressure amplitudes as the low draft sits in the more energetic part of the water column. It appears that in a scatter diagram of mixed seas the optimum shape is not the one with frequency matching but the one with highest forcing.

Fig. 5 shows the relationship between AAP per unit surface area with the buoy geometry, while Fig. 6 shows the same for AAP per unit displacement. Fig. 5 and Fig. 6 show that the buoys with the highest metrics are the very smallest, with the shallowest drafts and smallest radius. This result is relevant and reasonable since smaller buoys might well be expected to be more favourable for economic WEC development, with smaller buoys delivering higher energy-per-CAPEX; whether this remains the case once balance of plant and other costs required to combine WECs into a wave farm are considered is not considered here. However no local maximum is seen in these trends; see section VIII for further exploration of this observation.

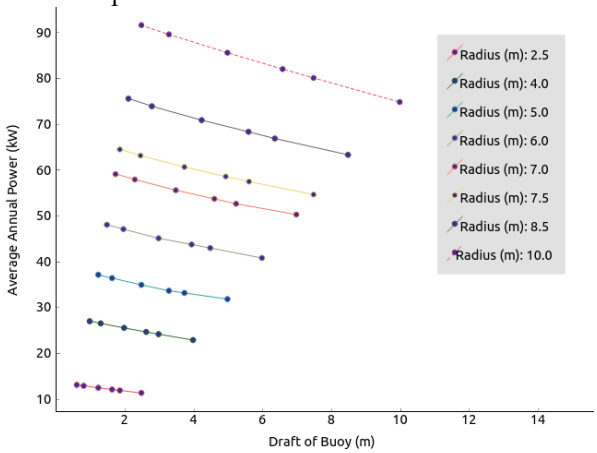

Fig. 4. AAP for buoys of various draft and radii.

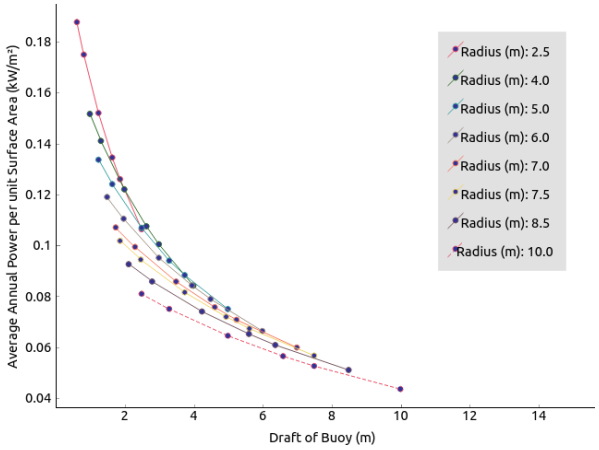

Fig. 5. AAP per unit surface area.

Fig. 7 and Fig. 8 give the graph of AAP per RMS PTO force, Fig. 7 gives draft on the x-axis while Fig. 8 gives radius. Both Fig. 7 and Fig. 8 plot the same underlying data. Fig. 7 shows the opposite trend to the AAP per unit displacement and AAP per unit surface area metrics. Fig. 8 shows a local maximum at around 6 to 7m radius for all draft values in our range. Fig. 8 is one of the few graphs in this work that shows a local maximum, see section VIII for further discussion. It is worth noting that the AAP for each of the permutations with highest AAP per RMS PTO Force is significantly lower than the maximum AAP for that geometry.

PTO stroke is likely a strong driver of PTO cost in some WEC designs, Fig. 9 shows the AAP per RMS PTO stroke. As was the case with AAP per unit displacement and per unit surface area the trend is downward, in this case however the denominator in the metric does not vanish as the draft goes to zero so the y-axis intercept can be expected to be finite. However, this result is no less problematic than AAP per unit displacement or per unit surface area. See section VIII for further discussion.

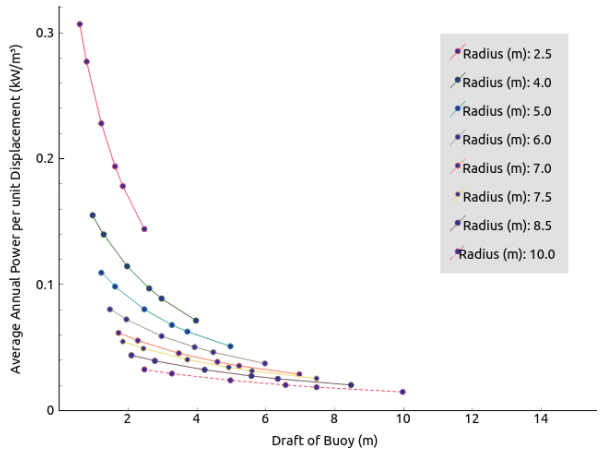

Fig. 6. AAP per unit displacement.

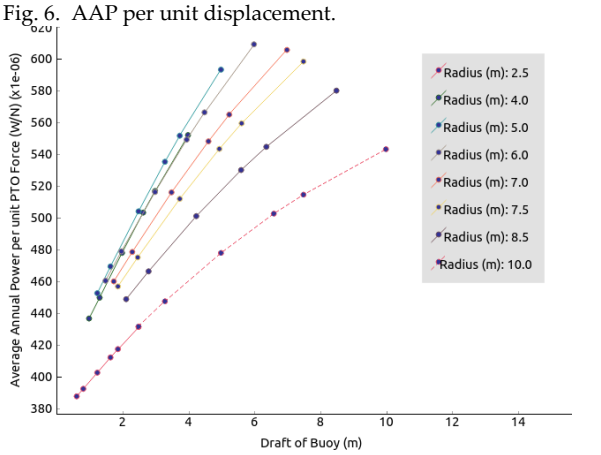

Fig. 7. AAP per RMS PTO effort against draft of buoy.

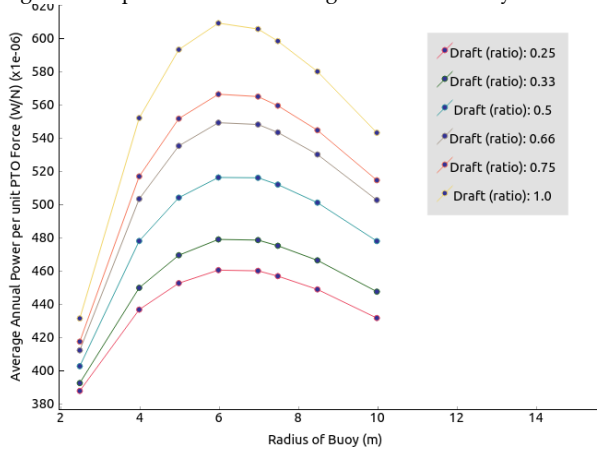

Fig. 8. AAP per RMS PTO effort against radius of buoy.

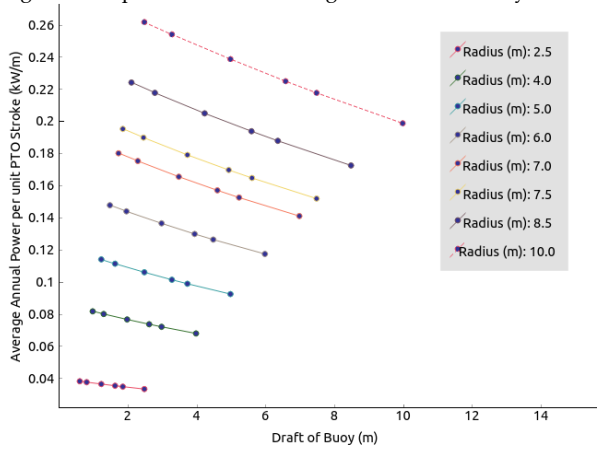

Fig. 9. AAP per unit RMS PTO Stroke.

L. Sub-surface buoy with seabed reaction

Similarly to the previous concept of the Surface Buoy with seabed reaction, the PTO was optimized for each geometry using the methodology outlined in section II. The sub-surface buoy is an ellipsoid and the parameters studied are the overall height of the ellipsoid and the horizontal radius. Fig. 10 shows the variation of AAP with height and radius of the sub-surface buoy. The AAP increases with height of buoy, this is due to the reduction in cancellation of excitation pressures due to opposite facing upper and lower surfaces exposed to in-phase Froude Krylov pressure due to incoming waves. This upwards trend can be expected to continue and ultimately level out when the lower surface of the buoy is below the waves and therefore attracts negligible dynamic pressure oscillations due to wave diffraction, and therefore no longer provides a partial cancellation of the downwards pressure on the upper surface.

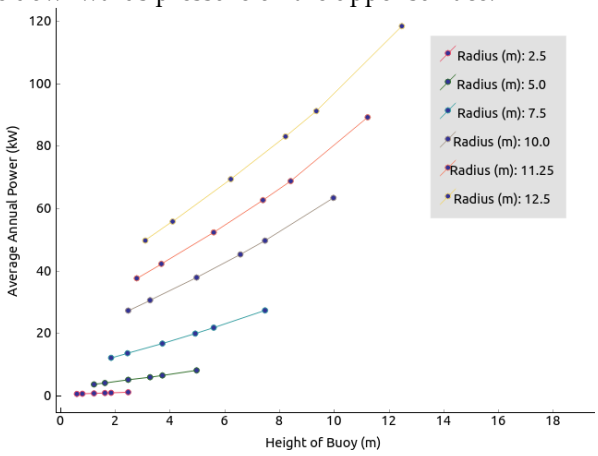

Fig. 10. Average Annual Power vs buoy height for a series of buoys of different radii.

The results in Fig. 11 to Fig 14 show how different metrics can be contradictory. Here, the largest buoys have the highest average annual power and the highest average annual power per unit surface area. But the best performing geometry per unit volume is the smallest, flattest buoy.

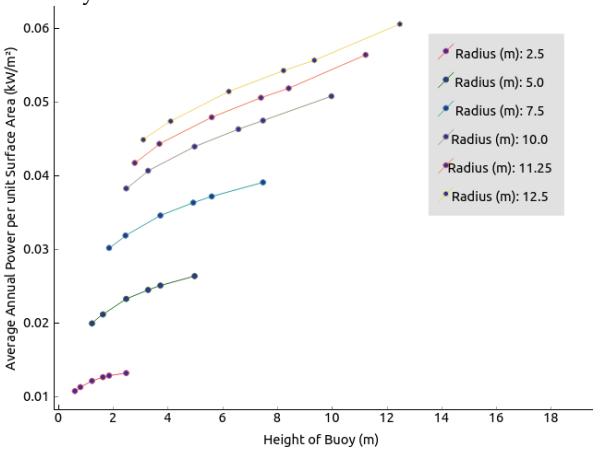

Fig. 11. AAP per unit Surface Area

Furthermore, the design with the highest ratio of AAP to displacement, (the smallest buoy radius 2.5 m, height 0.675 m) produced very little power. Given the high investment needed to install, moor, and connect WECs, it

is questionable that such low unit productivity is an optimal solution.

Note that the smallest buoys modelled here show very large motion amplitudes and large PTO stroke, relative to their size. It is likely that this would lead to some inaccuracy in the results in larger waves, as the linear model used here assumes movements are small. The motions of some of the instances will be outslde the linear range, see section VIII for further discussion.

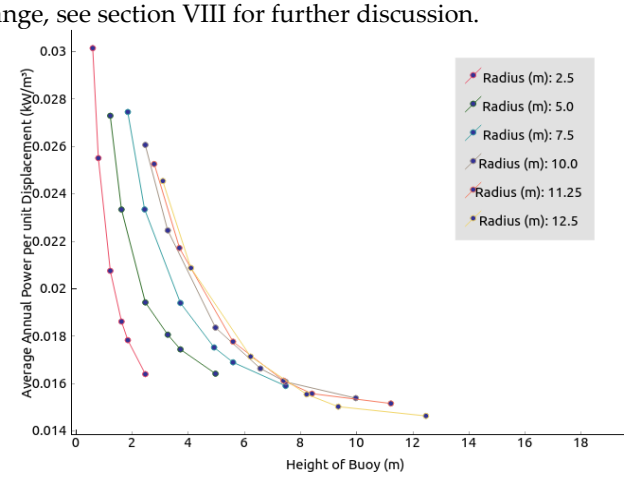

Fig 12. AAP per unit displacement

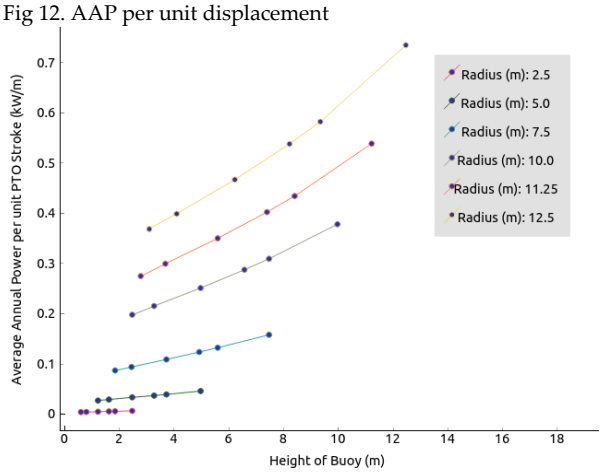

Fig 13. AAP per unit PTO Stroke

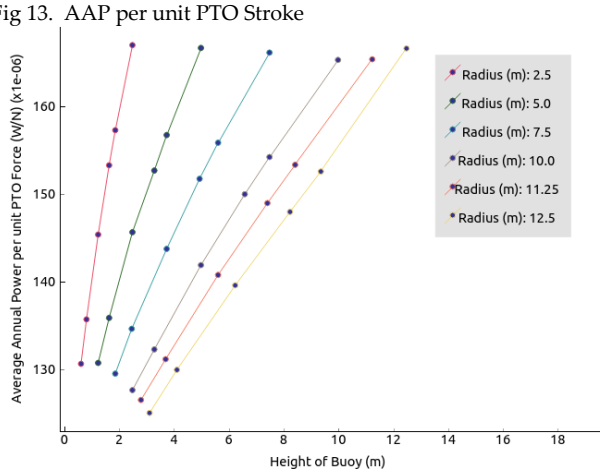

Fig 14. AAP per unit PTO force

M. Free-floating buoy with subsurface reaction plate

The device considered here shares the same surface piercing float considered in device *A* but here is connected to a circular sub-surface reaction plate instead of connected to the seabed. The parameter studies for this concept considered the radius of the submerged plate, and the depth to which it was submerged. The surface piercing body is fixed in size at 10m radius and 5m draft.

Fig. 15 shows the AAP for a range of radius and depth of reaction plate. The AAP increases with increasing submergence of the plate which suggests that excitation of the plate is not beneficial to the relative motion and that the performance can be expected to level out as submergence increases beyond the point where the wave forces on the plate are insignificant. The AAP is highest for plate radius approximately equal to the buoy radius. Fig. 16 to Fig. 19 show the selected metrics for various values of plate radius and submergence. In this instance each metric increases monotonically with increasing depth while AAP per unit surface area and AAP per unit displacement show a local maximum with respect to radius at plate radius approximately equal to buoy radius.

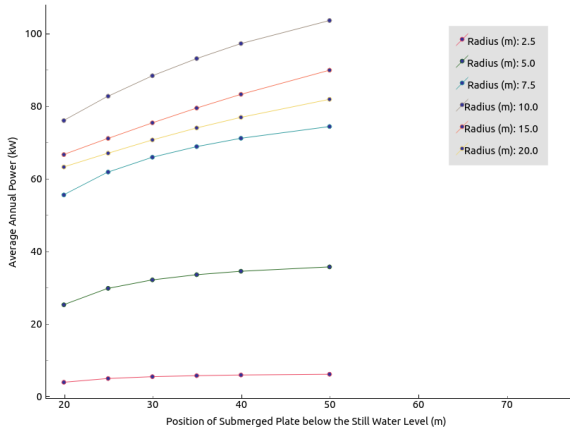

Fig. 15. AAP v depth of reaction plate

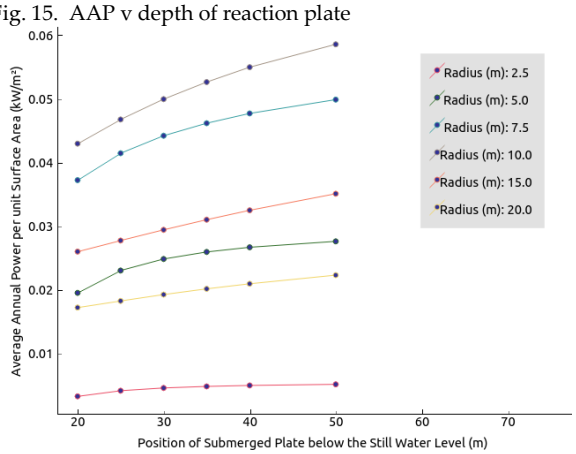

Fig. 16. AAP per unit surface area

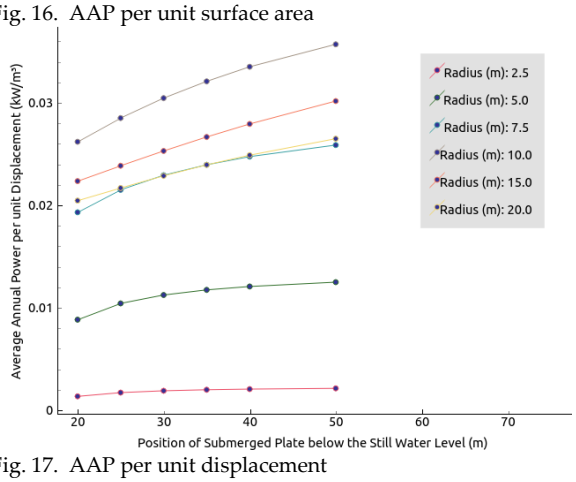

Fig. 17. AAP per unit displacement

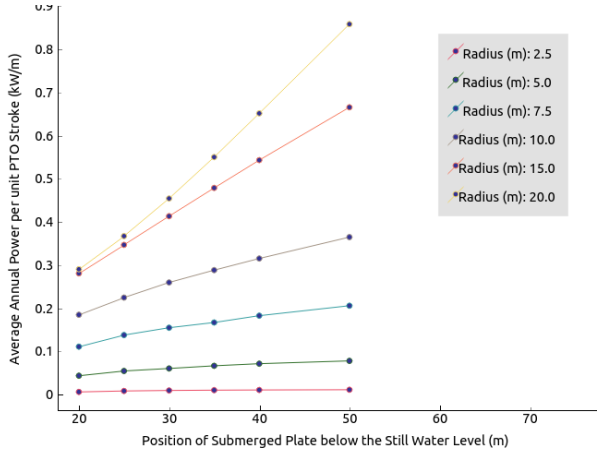

Fig. 18. AAP per RMS PTO stroke

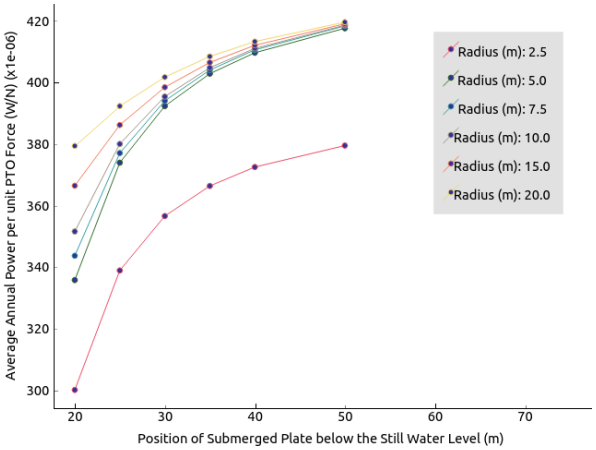

Fig. 19. AAP per RMS PTO force

N. Free-floating buoy with internal reaction mass

The device considered here shares the same surface piercing float considered in device *A* but here is connected to an internal sliding reaction mass instead of an external reaction plate or to the seabed.

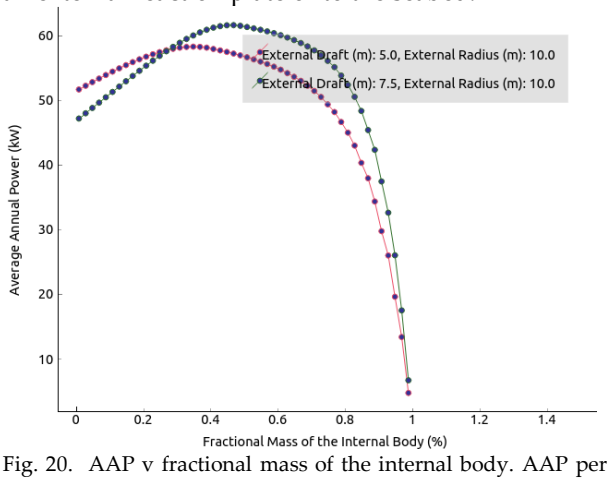

Fig. 20. AAP v fractional mass of the internal body. AAP per unit surface area and AAP per unit displacement will be scaled versions of this curve.

The PTO damping was optimised as for the other concepts. Fig. 20 shows the variation of AAP with mass split between the internal and external bodies for two different buoy draft values. Because the surface area and displacement of the buoy underlying each data series in Fig. 20 are constant the AAP per unit surface area and the AAP per unit displacement metrics will both be scaled versions of this graph.

Fig. 21 gives the AAP per RMS PTO force and Fig. 22 the AAP per RMS PTO stroke. These metrics give conflicting indications with AAP per unit PTO force reaching a local maximum at fractional mass values just under 1.0 while AAP per unit RMS PTO stroke is at a maximum when the fractional mass approaches zero.

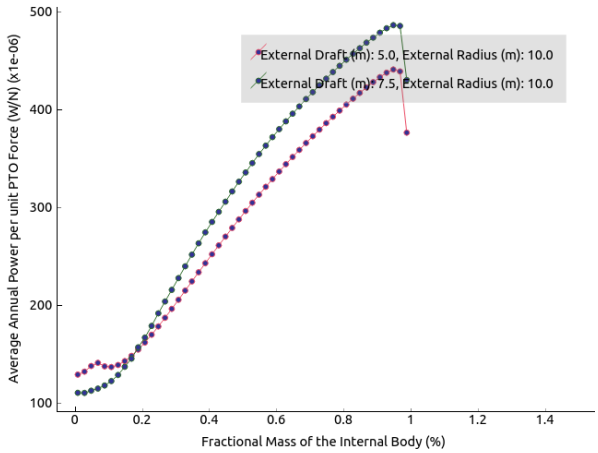

Fig. 21. Average Annual Power per RMS PTO Force

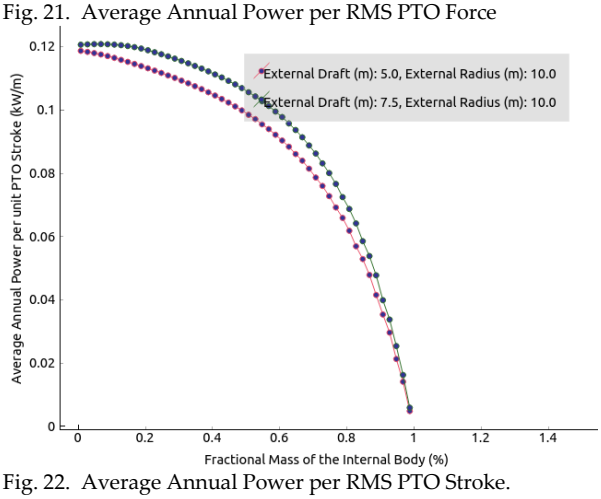

Fig. 22. Average Annual Power per RMS PTO Stroke.

O. Free-floating, two body axisymmetric WEC

The device considered here shares the same surface piercing float considered in device *A* but here is connected to second surface piercing float of rectangular toroidal shape rather than a fixed or other reaction frame. The two bodies are arranged coaxially so the overall device is axi-symmetric about its vertical axis. The PTO damping was optimised as described in section VIII. The shape of the central cylinder was held constant as was the inner radius of the toroid while the outer radius and draft of the toroid were studied.

Fig. 23 shows that the AAP increases with increasing outer radius of the toroid. However, as seen in Fig. 23, the relationship between AAP and draft is not constant, with increasing draft leading to an increase of AAP for smaller radii and to a decrease in AAP for larger radii. Fig. 24 to Fig. 26 give the relationship between the metrics introduced in section III and the geometry of the toroid. Note that in Fig. 24 and Fig. 25 the surface area and

displacement respectively are both for the combined 2 body system.

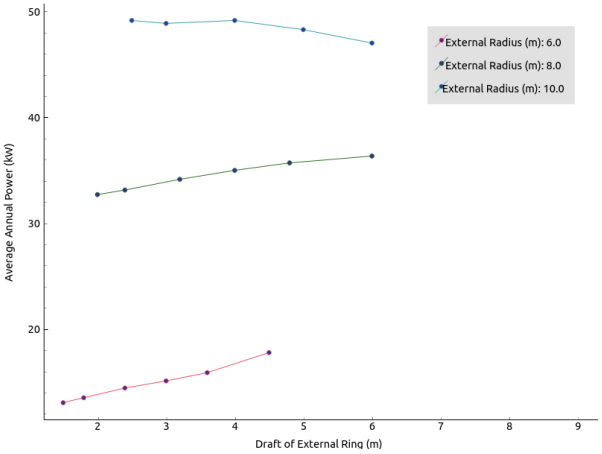

Fig. 23. AAP for various ring sizes.

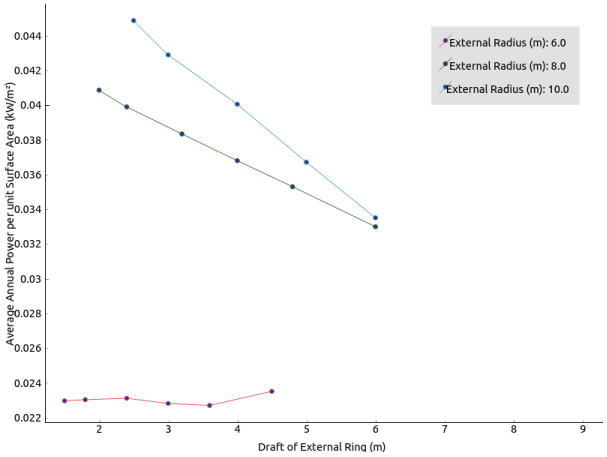

Fig. 24. AAP per unit Surface Area

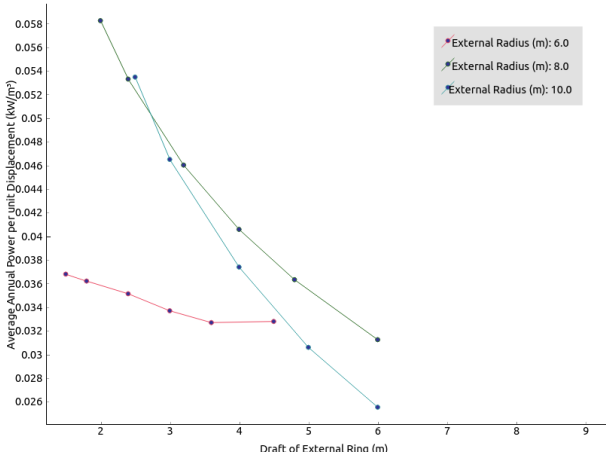

Fig. 25. AAP per unit displacement

The seemingly anomalous result for a toroid of radius 10m and draft 4m was retained to illustrate the misleading results from reliance on a single metric that can suggest optimal solutions which are in reality impractical. The difficulty seen with the AAP per unit PTO Force is that it will increase as the PTO force (and damping) decreases to zero, whereupon power is also extremely small. If the AAP yield for the permutations that resulted in the highest AAP per unit PTO force is contrasted to the maximum AAP of a geometry, then it is seen that optimising for AAP per unit PTO force leads to an AAP several orders of magnitude below the maximum. Whilst the optimal device is unlikely to be that with the highest AAP, it will not be one with such a low power yield. A similar difficulty is seen in the case of the AAP per RMS PTO metric.

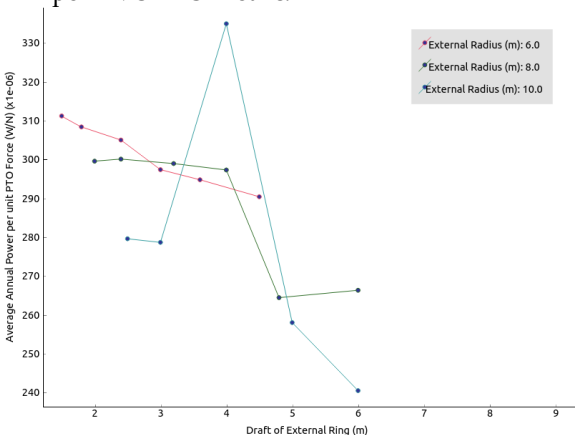

Fig. 26. Annual Average Power per RMS PTO Force

VI. POWER MATRICES OF DEVICES

Fig. 27 to Fig. 31 give the power matrices for the highest power instances of each device considered in this paper. No power cap has been applied to these matrices so caution should be exercised with regard to the higher values, in practice the rated power will correspond to a mid H_{m0} row in the figure, perhaps the highest power in the $H_{m0} = 3.5$m row. In addition no allowance for PTO efficiency or other power transmission losses has been made so these powers should be interpreted as raw absorbed power and not electrical power.

	Average Annual Power (kW)										
Significant Wave Height Hm0 (m)	Peak Period Tp (s)										
	3.5	4.5	5.5	6.5	7.5	8.5	9.5	10.5	11.5	12.5	13.5
0.5	0.0	0.2	0.8	1.8	3.0	4.1	5.1	5.8	6.3	6.6	6.7
1.5	0.3	2.0	7.3	16.2	26.8	37.1	45.8	52.4	56.8	59.2	60.2
2.5	0.7	5.6	20.2	44.9	74.4	103.1	127.3	145.5	157.6	164.6	167.3
3.5	1.4	10.9	39.6	88.0	145.9	202.2	249.6	285.2	309.0	322.5	327.8
4.5	2.3	18.0	65.5	145.4	241.1	334.2	412.6	471.4	510.8	533.2	541.9
5.5	3.4	26.9	97.9	217.2	360.2	499.2	616.3	704.2	763.0	796.4	809.6
6.5	4.8	37.5	136.7	303.4	503.1	697.3	860.8	983.6	1065.7	1112.4	1130.7

Fig. 27. Power matrix for a surface buoy of radius 10m and draft 2.5m.

	Average Annual Power (kW)										
Significant Wave Height (m)	Time Period (Tp)										
	3.5	4.5	5.5	6.5	7.5	8.5	9.5	10.5	11.5	12.5	13.5
0.5	0.04	0.47	1.69	3.45	5.23	6.68	7.64	8.13	8.22	8.03	7.66
1.5	0.32	4.23	15.24	31.02	47.05	60.09	68.77	73.14	73.98	72.29	68.95
2.5	0.89	11.75	42.34	86.16	130.71	166.92	191.02	203.16	205.51	200.81	191.52
3.5	1.74	23.04	82.98	168.87	256.18	327.17	374.40	398.19	402.81	393.58	375.39
4.5	2.88	38.08	137.17	279.16	423.49	540.83	618.90	658.23	665.86	650.62	620.53
5.5	4.31	56.89	204.91	417.01	632.62	807.91	924.54	983.28	994.68	971.91	926.97
6.5	6.01	79.46	286.20	582.44	883.58	1128.40	1291.29	1373.35	1389.27	1357.47	1294.70

Fig. 28. Power matrix for a submerged buoy of radius 12.5 m and height 12.5 m.

	Average Annual Power (kW)										
Significant Wave Height (m)	Wave Period, Tp (s)										
	3.5	4.5	5.5	6.5	7.5	8.5	9.5	10.5	11.5	12.5	13.5
0.5	0.01	0.12	0.60	2.00	4.36	6.56	7.71	7.79	7.21	6.34	5.42
1.5	0.13	1.07	5.41	18.03	39.20	59.01	69.35	70.13	64.92	57.09	48.77
2.5	0.36	2.97	15.02	50.08	108.89	163.90	192.64	194.81	180.33	158.58	135.47
3.5	0.71	5.83	29.44	98.16	213.43	321.25	377.58	381.84	353.45	310.83	265.52
4.5	1.17	9.64	48.66	162.27	352.82	531.05	624.17	631.20	584.27	513.81	438.92
5.5	1.75	14.40	72.69	242.40	527.05	793.29	932.40	942.90	872.80	767.55	655.68
6.5	2.45	20.11	101.53	338.56	736.13	1107.99	1302.27	1316.95	1219.03	1072.03	915.78

Fig. 29. Power Matrix for a Surface buoy with submerged reaction plate of radius 10m at a depth of 50m

Significant Wave height (m)	IRM	Average Annual Power (kW)										
		3.5	4.5	5.5	6.5	7.5	8.5	9.5	10.5	11.5	12.5	13.5
	0.5	0.00	0.02	0.33	1.50	3.11	4.21	4.55	4.37	3.94	3.43	2.95
	1.5	0.00	0.21	2.99	13.52	28.03	37.88	40.93	39.30	35.44	30.91	26.51
	2.5	0.01	0.58	8.31	37.56	77.86	105.22	113.69	109.16	98.43	85.86	73.64
	3.5	0.02	1.14	16.28	73.62	152.61	206.24	222.82	213.95	192.93	168.28	144.33
	4.5	0.03	1.88	26.92	121.70	252.27	340.93	368.34	353.67	318.92	278.18	238.59
	5.5	0.04	2.81	40.21	181.80	376.84	509.29	550.24	528.32	476.41	415.56	356.41
	6.5	0.06	3.92	56.16	253.92	526.33	711.32	768.51	737.91	665.40	580.41	497.80

Fig. 30. Power Matrix for a body of radius 10m and draft 7.5m with an Internal Mass Fraction of 50% at optimum PTO damping

Significant Wave Height (m)		Average Annual Power (kW)										
		Time Period, Tp (s)										
		3.5	4.5	5.5	6.5	7.5	8.5	9.5	10.5	11.5	12.5	13.5
	0.5	0.07	3.71	10.70	11.68	9.51	7.13	5.29	4.00	3.09	2.46	2.01
	1.5	0.64	33.38	96.27	105.14	85.63	64.19	47.65	35.96	27.82	22.13	18.06
	2.5	1.79	92.73	267.42	292.05	237.85	178.31	132.36	99.88	77.29	61.46	50.17
	3.5	3.51	181.76	524.14	572.42	466.19	349.49	259.42	195.76	151.49	120.46	98.33
	4.5	5.80	300.46	866.44	946.24	770.65	577.73	428.84	323.60	250.42	199.13	162.55
	5.5	8.66	448.83	1294.31	1413.52	1151.21	863.03	640.62	483.40	374.09	297.46	242.83
	6.5	12.09	626.88	1807.76	1974.25	1607.89	1205.39	894.75	675.16	522.48	415.46	339.16

Fig. 31. . Power Matrix for a two-body axisymmetric WEC with a ring diameter of 10 m and a ring draft of 7.5 m

VII. Results Summary

TABLE 1 COMPARISON OF BEST METRIC VALUES

Concept	AAP (kW)	AAP/SA (kW/m²)	AAP/DIS (kW/m³)	AAP/PTO FORCE (W/N)	AAP/PTO STROKE (kW/m)
A	91.55 radius = 10.0m; draft = 2.5m	187.69 radius = 2.5m; draft = 0.625	306.52 radius = 2.5m; draft = 0.625	0.609 radius = 6m; draft = 1m	261.62 radius = 10m; draft = 2.5m
B	118.30 radius = 12.5m; draft = 12.5m	60.56 radius = 12.5m; draft = 12.5m	30.13 radius = 2.5m; draft = 0.625m	0.167 radius = 2.5m; draft = 2.5m	734.19 radius = 12.5m; draft = 12.5m
C	103.58 plate radius = 10 m; plate depth = 50 m	58.58 plate radius = 10m; plate depth = 50m	35.71 plate radius = 10m; plate depth = 50m	0.420 plate radius = 20m; plate depth = 50m	858.40 plate radius = 20m; plate depth = 50m
D	61.62 radius = 10.0m; draft = 7.5m; internal mass fraction = 47%	41.89 radius = 10m; draft = 5.0m; internal mass fraction = 25%	16.02 radius = 10.0m; draft = 5m; internal mass fraction = 33%	0.486 radius = 10.0m; draft = 7.5m; internal mass fraction = 95%	120.74 radius = 10m; draft = 7.5m; internal mass fraction = 7%
E	104.71 radius = 10.0m; draft = 7.5m	68.36 radius = 10.0m; draft = 7.5m	58.25 radius = 8.0m; draft = 2.0m	0.969 Radius = 10m; draft = 7.5m	1481.22 radius = 10m; draft = 7.5m

Table 1 summarises the metric results for all concepts. That the metrics predict contradictory optimal geometries is apparent, and the reasons for this have been discussed in previous sections. To summarise this, the main cause of discrepancies between metrics is not that they predict incorrect optima but that real-world considerations not included in each metric reduce its applicability. The metrics did not consider the balance of plant costs or a minimum power production for optimal geometries, and so those that considered device size were often led to recommend the smallest buoys which in practice most likely would not be economical.

As Table 2 shows, there is no concept for which all the metrics show a consistent trend. From this, it is concluded that a robust analysis should consider several metrics, or at the very least consider a single metric for several geometries with a strong awareness of the limitations of the metric chosen. This would increase the usefulness of early stage device modelling and prevent false confirmation of geometries which provide a local maximum only in one metric.

Furthermore, the metric trends in some cases suggest optimum geometries that are infeasible, such as buoys of zero volume, or are beyond the limitations of the model, such as smaller buoys with large movements.

Both optimisation issues could be avoided with a more general model, which considers several metrics and applies stricter sanity conditions to the optimisation.

TABLE 2 COMPARISON OF TRENDS IN METRIC GRAPHS

Device (x-axis variable)	AAP	AAP / Surf. Area	AAP / Displ'	AAP / RMS PTO Stroke	AAP / RMS PTO Force
A (draft of buoy)	↓	↓	↓	↑	↓
A (radius of buoy)	↑	↓	↓	↑	Local max
B (height of ellips')	↑	↓	↑	↑	↑
B (radius of ellips')	↑	↑	↑*	↑	↓
C (depth of plate)	↑	↑	↑	↑	↑
C (radius of plate)	Local max	Local max	Local max	↑	↑
D (mass fraction)	Local max	Local max	Local max	↑	↓
D (draft)	↑	↑	↑	↑	↑
E (draft of toroid)	↑	↓	↓	↓	↓
E (radius of toroid)	↑	↑	↑	Unclear	Unclear

VIII. Conclusion

A multi concept, multi instance, multi metric comparative study has been presented.

The overall conclusion is that none of the metrics considered are universally suitable for use as the objective function in an automatic optimisation.

Very few metric v geometric parameter curves show a local maximum, most are monotonically increasing or decreasing. Most likely the increasing graphs will reach a local maximum outside the range of parameters tested here. The decreasing curves in particular are problematic since allowing an optimisation to follow these curves leads to zero volume/area/stroke geometries.

All of the metrics bar AAP have infinite values when the displacement, surface area, PTO damping and PTO stroke approach zero faster than the power does (or if the power does not approach zero) as any geometric parameter is varied. Draft of a floating body is an example of a parameter with this property. These metrics are unsuitable for use in optimisations of such parameters. This problem is a consequence of the optimization leading to designs for which the underlying modelling technique is invalid. To avoid this a more general simulation model is needed or intensive human supervision of the optimization needs to be maintained.

A further possible weakness in metrics that favour smaller WEC designs (e.g. AAP per displacement) is that they promote low unit powers. It is likely that this will not lead to an optimal solution when the costs of balance of plant and especially moorings and electrical connections are fully considered. This consideration suggests that device optimisation must include farm level considerations.

The smallest buoys modelled often show motion amplitudes greater than their dimensions, a modelling approach that enforces the Budal-limit would be beneficial and would lead to different results.

In many cases different metrics gave contradictory indications. In the case of the sub surface buoy device AAP per unit surface area and AAP per unit displacement give contradictory indications with respect to the best choice of buoy height. In several of the concepts AAP per RMS PTO force and AAP per RMS PTO stroke also give contradictory indications.

Contradictory indications can be seen as following from different sets of real-world considerations included in each metric and, importantly, different sets of real-world considerations that are omitted from each metric and so limit its applicability.

A possible way to overcome the difficulty of these contradictory indications is to combine multiple metrics in a weighted average or in a nonlinear combination that allows the real world metric to better reflects the realities that are only partially reflected in the individual metrics.

For device type A wider and shallower buoys have the greatest average annual power. This result for the whole scatter annual average power is contrary to results calculated for power in monochromatic waves which would favour higher drafts in order to promote resonance. (The result is most likely only applicable to neutrally buoyant structures and not applicable to devices that use negative spring to reduce natural frequency and increase heave motion).

For device type D where the outer hull is fixed and an inner reaction mass is optimised the AAP per unit surface area and AAP per unit displacement are effectively the same metric as AAP since the denominator of the metrics is fixed.

REFERENCES

[1] R. Costello and A. Pecher, "Ch5: Economics of WECs," in *Handbook of Ocean Wave Energy*, Springer, 2017, pp. 101-139.

[2] A. Babarit, J. Hals, M. Muliawan, A. Kurniawan, T. Moan and J. Krokstad, "Numerical benchmarking study of a selection of wave energy converters," *Renewable Energy*, vol. 41, pp. 44-63, 2011.

[3] EMEC, "Wave Devices," 3 February 2017. [Online]. Available: http://www.emec.org.uk/marine-energy/wave-developers/. [Accessed 12 December 2018].

[4] R. Costello, "Horizon Scanning for Commercial Wave Energy Technology," in *EWTEC*, Cork, 2017.

[5] K. Gürsel, D. Ünsalan, G. Neser, M. E. Taner and M. Önal, "A Technological Assessment of the Wave Energy Converter," *Naval Academy Scientific Bulletin*, vol. XIX, no. Issue 1, pp. 408 - 417, 2016.

[6] J. Falnes, Ocean Waves and Oscillating Systems, Cambridge: Cambridge University Press, 2002.

[7] M. Alves, "Frequency-Domain Models," in *Numerical Modelling of Wave Energy Converters*, M. Folley, Ed., London, Elsevier, 2016, pp. 11-30.

[8] Wave Venture, "Wave Venture Theory Manual," 2019.

[9] A. Babarit and G. Delhommeau, "Theoretical and numerical aspects of the open source BEM solver NEMOH," in *11th European Wave and Tidal Energy Conference*, Nantes, France, 2015.

[10] M. Alves, "Frequency Domain Models," in *Numerical Modelling of Wave Energy Converters*, M. Folley, Ed., London, Elsevier, 2016, pp. 23-25.

[11] D. P. Dee, S. M. Uppala, A. J. Simmons, P. Berrisford, P. Poli, S. Kobayashi, U. Andrae, M. A. Balmaseda, G. Balsamo, P. Bauer, P. Bechtold, A. C. M. Beljaars, L. van de Berg, J. Bidlot, N. Bormann, C. Delsol, R. Dragani, M. Fuentes, A. Geer, L. Haimberger, S. Healy, H. Hersbach, E. Holm, L. Isaksen, P. Kallberg, M. Kohler, M. Matricardi, A. McNally, B. Monge-Sanz, J. Morcrette, B.-K. Park, C. Peubey, P. de Rosnay, C. Tavolato, J.-N. Thepaut and F. Vitart, "The ERA-Interim reanalysis; configuration and performance of the data assimilation system," *Q.J.R Meteorological Society*, no. 137, pp. 553-597, 2011.

[12] J. Falnes and H. J, "Heaving buoys, point absorbers and arrays," *Philosophical Transactions of the Royal Society A*, vol. 370, no. 1959, pp. 246-277, 2012.

[13] N. Sergiienko, B. Cazzolato, B. Ding, P. Hardy and M. Arjomandi, "Performance comparison of the floating and fully submerged quasi-point absorber wave energy converters," *Renewable Energy*, vol. 108, pp. 425-437, 2017.

[14] M. Vantorre, R. Banasiak and R. Verhoeven, "Modelling of hydraulic performance and wave energy extraction by a point absorber in heave," *Applied Ocean Research*, vol. 26, pp. 61-72, 2004.

[15] K. Koca, A. Kortenhaus, H. Oumeraci and B. Zanuttigh, "Recent Advances in the Development of Wave Energy Converters," in *EWTEC 2013*, Aalborg, 2013.

[16] C. Liang and L. Zuo, "On the dynamics and design of a two-body wave energy converter," *Renewable Energy*, vol. 101, pp. 265-274, 2017.